FINAL VERSION BEFORE EDITORIAL: IEEE TRANSACTIONS ON SMART GRID, VOL. 3, NO. 4, DECEMBER 2012

Real-Time Central Demand Response for Primary Frequency Regulation in Microgrids

S.A. Pourmousavi, *Student Member, IEEE,* M.H. Nehrir, *Fellow, IEEE*

***Abstract*—Providing ancillary services for future smart microgrid can be a challenging task because of lack of conventional automatic generation control (AGC) and spinning reserves, and expensive storage devices. In addition, strong motivation to increase the penetration of renewable energy in power systems, particularly at the distribution level, introduces new challenges for frequency and voltage regulation. Thus, increased attention has been focused on demand response (DR), especially in the smart grid environment, where two-way communication and customer participation are part of. This paper presents a comprehensive central DR algorithm for frequency regulation, while minimizing the amount of manipulated load, in a smart microgrid. Simulation studies have been carried out on an IEEE 13-bus standard distribution system operating as a microgrid with and without variable wind generation. Simulation results show that the proposed comprehensive DR control strategy provides frequency (and consequently voltage) regulation as well as minimizing the amount of manipulated responsive loads in the absence/presence of wind power generation.**

***Index Terms*—Adaptive hill climbing, ancillary service, demand response, microgrid, smart grid, step-by-step control.**

I. Introduction

DEMAND Response (DR) offers a variety of financial and operational benefits for electricity customers, load-serving entities (whether integrated utilities or competitive retail providers) and grid operators [1]. In particular, DR can be an effective tool in providing balance between supply and demand in real-time. Traditionally, such services, known as ancillary services, are provided by utility-owned operating (spinning and non-spinning) reserves which are basically flexible capacity generators, available when needed, to maintain secure operation of power systems. From an economic perspective, these services and reserve power are costly and any method which manages to reduce the magnitude of these services, without sacrificing system stability, is of significant importance [1], [2].

Intermittent renewable power generation, such as wind and photovoltaic (PV), are projected to take a considerable share of future power generation, as distributed generation (DG) sources, installed at the distribution level. In order to compensate for the highly variable generation, more spinning and non-spinning reserve are necessary in the future which introduces new costs and more pollution, associated with the conventional power plants. These problems will increase in intensity and occurrence in the case of islanded microgrids, where no conventional ancillary services are technically available. Thus, more expensive storage devices will be necessary to provide reliable electricity to customers with acceptable quality. These challenges and uncertainties make DR a viable option—DR resources provide a reliable, low cost, environmentally-friendly alternative to conventional spinning reserves. DR can also provide ancillary services which grid operators—independent system operators (ISOs), regional transmission organizations (RTOs) or utilities—and other entities can use [2]. These entities can control customer controllable loads to shift or reduce their load profile or respond to excess or insufficient renewable generation.

Demand resources are specifically defined as a subset of non-spinning reserves and must be available within 10 minutes or shorter from the time they are called upon [2]. When the demand resources are controlled immediately upon the occurrence of disturbances, the strategy is often called direct load control (DLC). This capability can be technically and economically achieved through responsive electric devices such as electric water heaters (EWHs) equipped with hot water storage tank [3]-[5]. On the average, residential EWHs electricity consumption accounts for about 11% of the total electricity consumption and increases to over 30% during peak demand hours [4], [6]. Therefore, there is a considerable potential for EWHs to be effective in DR applications for providing ancillary services.

Although it may seem likely that the individual demand resources may have a high failure rate to curtail load on short notice, the aggregation of many small resources into one large resource makes it more probable that the assigned response will be achieved. This characteristic of demand resources potentially makes DR resources more reliable than conventional generation, where the failure of one generator to start can cause the loss of considerable spinning reserve capacity [1], [2].

Considerable attention has recently been given to DR for different purposes. The economic benefits of DR in the power market and the development of strategies to achieve such benefits are reported in [7]-[11]. DR has also been used for off-line planning and day-ahead scheduling, e.g. [12]-[17]. The availability of load as DR resource for reserve capacity (ancillary services market) has been investigated in [18]-[20]. However, these references do not examine the effect of DR on

This work was in part supported by Pacific Northwest National Laboratory (PNNL), which is operated for the U.S. Department of Energy by Battelle under Contract DE-AC05-76RL01830, and by the DOE Award DE-FG02-11ER46817.

S.A. Pourmousavi (e-mail: s.pourmousavikani@msu.montana.edu), M.H. Nehrir (e-mail: hnehrir@ece.montana.edu) are with the Electrical and Computer Engineering Department, Montana State University, Bozeman, MT 59717 USA.

system frequency nor do they model the transmission or distribution grid. A limited number of studies also address the effectiveness of decentralized dynamic demand control on stabilization of grid frequency, mainly at the transmission level [18][21]-[24]. This paper presents a central DR strategy for primary frequency regulation in a microgrid at the distribution level, which is considered as a cornerstone of the future smart grid. The details of the proposed DR strategy are given below.

A comprehensive DR strategy has been designed by the authors to continuously balance generation and demand, using an adaptive hill climbing (AHC) strategy [25], which results in frequency regulation. The AHC control is then replaced with a step-by-step (SBS) controller to reduce the amount of manipulated load to a minimum at steady-state [26]. In these references, the designed strategies were tested on a very small (one-bus) system to show the proof of concept. The novelties and contributions of this paper (not reported in [25]and [26]) are as follows:

- The DR strategy is applied to a realistic (a standard IEEE 13-bus) distribution system operating as an independent microgrid, which shows the effect of DR on the system frequency, [10]. Because of high R/X ratio at the distribution level, the frequency regulation also results in voltage regulation.
- A decision tree is presented to accurately determine the operation mode of the controller.
- The effectiveness of the DR strategy is evaluated under the presence of variable wind-generated power to show its ability for generation following to regulate the system frequency.
- The impact of communication delay (latency) in the performance of the DR strategy is evaluated.

Simulation results show the effectiveness of the DR approach in providing frequency (and consequently voltage) regulation in the presence and absence of wind power generation. The dynamic models of the islanded microgrid are developed in MATLAB/Simulink®.

The rest of the paper is organized as follows: Section II describes the proposed comprehensive DR strategy comprising of AHC and SBS controllers. System of study and simulation setup is explained in Section III. Simulation results for different scenarios with and without wind power generation are shown and discussed in Section IV. Section V presents a discussion about the latency and its impact on the results. Finally, conclusions of the study are given in Section VI.

II. The Proposed DR Strategy

In general a DR management involves four main participants: 1) the balancing authority, which includes the DR initiator and the entity having interest in this service, namely the utility. The central controller proposed in this paper is assumed to be owned by this balancing authority; 2) a DR aggregator (which integrates the individual DR resources); 3) the distribution utility (that operates the distribution feeders); and finally 4) the customers (energy consumers who participate in the DR program) [10]. Any DR scheduling process starts from the balancing authority, which determines and requests (announces) the volume of DR required at any given time [10]. This type of DR lies within the incentive-based program (IBP) of DR [27]. Although this structure can be used for all three frequency regulation services including the primary, secondary and tertiary regulations, this paper only deals with the primary frequency control. In this process, active power of the generating units and the consumption of controllable loads are adjusted to quickly balance the load and generation and restore the frequency [28]. In this way, every balancing authority center needs a calculation center with a DR strategy to determine the amount of required DR to regulate the frequency based on the system frequency deviation. The focus of this paper is to solve this issue by introducing a comprehensive DR strategy, which is based on feedback of the frequency deviation, to regulate the system frequency in real time. This process is shown in Fig. 1

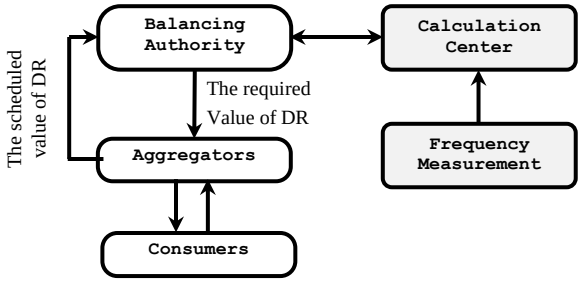

Fig. 1. The scheduling process of the central DR strategy.

The proposed DR strategy, referred to as central direct load control (CDLC), consists of three operation modes depending on the magnitude of the system frequency deviation (△f), as shown in Fig. 2. The figure shows a hypothetical curve of △f vs. time, where three operation modes (0, 1, and 2) are shown as follows:

✓ MODE 0: Normal operation-no control needed.

✓ MODE 1: In this mode, △f goes out of the desired range, and load control is applied to bring △f within the range with maximum effort, as quickly as possible. The AHC control [25] is applied in this operation mode.

✓ MODE 2: In this mode, the frequency has returned to the normal range, and the SBS load manipulation strategy is used to minimize the amount of manipulated load [26]. We will call the combination of the above three steps "comprehensive control".

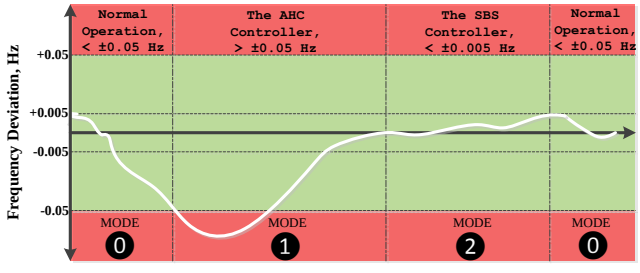

Fig. 2. Concept of the proposed control strategy.

The conditions for the three operation modes discussed above are given in the decision tree shown in Fig. 3. In this figure, △f_der is the 1st-order derivative of frequency

deviation with respect to time, abs is the absolute operator, and AND/OR are the logical and/or operators, respectively. The decision tree gives the required conditions which must be satisfied for the three operation modes. Checking the derivative of the system frequency deviation at every sample in MODEs 1 and 2 (to precisely determine the transition from one mode to the other) is required to assure stable operation of the system. MODE 1 will begin once the system frequency deviation exceeds 0.05 Hz, if the system has previously been in MODE 0. MODE 1 will continue as long as $\Delta f\_der \neq 0$. MODE 2 will take over the control of the system if the following three conditions hold true: 1) $abs(\Delta f) < 0.005$ Hz, 2) $\Delta f\_der = 0$, and 3) the system has been in MODE 1 in the previous iteration. This mode of operation will remain active as long as $\Delta f\_der \neq 0$ and $abs(\Delta f) < 0.005$ Hz, if the system was in MODE 2 in the previous iteration. MODE 0 takes over if $abs(\Delta f) > 0.005$ and the system has been operating in MODE 2. This mode will continue as long as $abs(\Delta f) < 0.05$ and the system was in MODE 0 in the previous iteration.

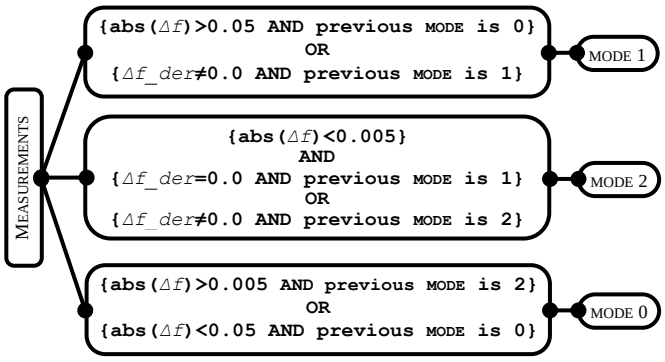

Fig. 3. Decision tree for determining the mode of operation

The 0.05 and 0.005 frequency deviations used in Fig. 3 are based on 60-Hz operation used in North America [27]. The AHC and SBS load control strategies used in operation MODEs 1 and 2, respectively, are explained in subsections II.A and II.B.

In North America, whenever a frequency error persists for a certain time (10 seconds for the east, 3 seconds for Texas, and 2 seconds for the west), a correction of ±0.02 Hz (0.033% of 60 Hz) is applied [28]. In this study, if frequency deviations reach 0.5 Hz, automatic load shedding or other control actions are used to restore system frequency. In addition, the time and magnitude effect is integrated in a desired dead-band of ±0.05 Hz (0.083% of 60 Hz) for this study. That is, when frequency deviation exceeds ±0.05 Hz under a disturbance (Fig. 2), the AHC controller will start operating to regulate the frequency by changing the amount of responsive loads. Once the AHC controller has brought the frequency within the ±0.005 Hz limit, the SBS controller becomes active to minimize the amount of manipulated load.

A. Adaptive Hill Climbing Control

The flowchart of the AHC controller (operating MODE 1) is shown in Fig. 4. The frequency, measured at the point of common coupling (PCC) of the microgrid, is the input variable to the controller. At each time step *k*, if the frequency deviation falls outside the dead-band (i.e., if $abs(\Delta f) > 0.05$ Hz), the percentage of the responsive load (that will turn ON or OFF) is computed as follows:

$$\%Load(k) = \%Load(k-1) + \Delta f \times M \quad (1)$$

where *%Load(k-1)* is the percentage of manipulated load at time step *k-1*, and $\Delta f \times M$ is a perturbation parameter. M is a constant used to scale down the frequency deviation. In this study, after several simulation runs under different loading conditions, M was set to 0.1, which gave the most satisfactory result.

When the frequency is higher than acceptable ($\Delta f > 0.05$), a percentage of the responsive loads (that are OFF) will turn ON, and when it is lower than acceptable ($\Delta f < -0.05$), a percentage of the responsive loads (that are ON) will turn OFF. This procedure is adaptive since the amount of manipulated load is a function of the frequency deviation, which tends to reduce the deviation with maximum effort. More detail on the AHC algorithm is provided in [25].

The AHC controller acts faster than the speed governor of the diesel generator because of the rapid nature of control, since the power consumption status of controllable loads (such as EWHs and other resistive loads) can be changed instantaneously by the ON or OFF command signal they receive. This way, more responsive loads will be manipulated at the beginning of the disturbances (in an attempt to bring the frequency within the desired limit as quickly as possible) than required at steady-state.

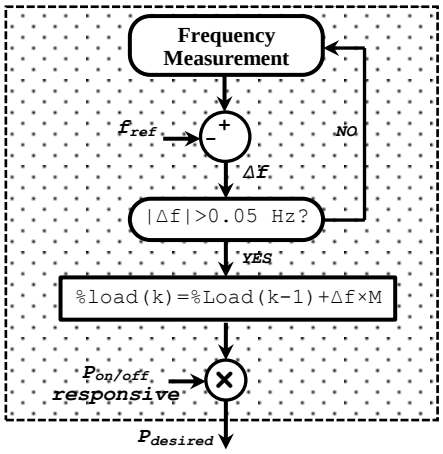

Fig. 4. The flowchart of the AHC control [25].

As a result, a higher percentage of the responsive loads are manipulated at steady-state, which maybe more than needed. Because of this, a SBS controller was designed, [26], to reduce the amount of manipulated loads to a minimum at steady-state. The operation of this controller is explained in the next subsection.

B. Step-by-step Control

In order to assure that the minimum required amount of responsive load is activated (kept ON or OFF) at steady-state, the SBS control (MODE 2), introduced in Fig. 2, is used. Once the frequency is stabilized by the AHC controller, the SBS controller will start operating to minimize the amount of

manipulated responsive loads. In order to assure safe operation of the system, the SBS will act in a smaller dead-band (abs(Δf)<0.005 Hz), as shown in Fig. 2. Using the SBS controller, the manipulated responsive load will be decreased by 5% at each one-second time-step according to Eq. (2), until the frequency begins to go out of the desired dead-band.

$$\%Load(k) = 0.95 \times \%Load(k-1) \quad (2)$$

According to Eq. (2), the responsive load variation depends on its previous value. Therefore, the load control strategy begins with large variations in load which decrease with time. The SBS control strategy is therefore non-linear with large load variations at the beginning and small ones at the end. As a result, the proposed control strategy minimizes the amount of responsive loads that need to be manipulated at steady-state to keep the system frequency within the desired range of ±0.05 Hz. The advantage of the SBS strategy is that a lower percentage of responsive loads is manipulated at steady-state, which improves customers' quality of service (QoS). As a result of this improvement, a higher percentage of customer loads will be available for future control, if needed.

III. Study System

To verify the effectiveness of the comprehensive controller designed, it was applied to an IEEE standard 13-bus distribution network, [30] and [31], shown in Fig. 5. This feeder is assumed to be the distribution system company in the structure introduced in section II, as shown in Fig. 1. However, to be able to observe the frequency behavior of the system as a microgrid, the utility source of the original model was replaced with a 15-MW diesel DG and a variable load which can be adjusted to set the DG's operating point (e.g., to light or heavy loading). The DG is equipped with a speed governor and excitation system whose parameters are given in the Appendix. A 1-MW dump load is also added to the 69-kV bus. This load is only enabled in light loading conditions (in the no-control case) to prevent the frequency deviation from exceeding 0.5 Hz.

A 2-MW wind turbine (about 30% of the system load), shown in Fig. 5, is added to the system (at the PCC) in order to study the effect of the proposed comprehensive controller on a realistic distribution system with high penetration of wind power. To observe the system frequency deviation, the maximum mechanical torque of the diesel generator has been limited to a certain point for each simulation case studied. The limit for each case is given in the simulation results.

The dynamic model for the diesel engine (with speed governor, excitation controller and synchronous generator) is extracted from MATLAB/Simulink SimPowerSystems toolbox [32], which is based on IEEE standard 421.5 [33].

It is desired to have a model of the load where active power (P) would explicitly vary during the simulation. Such a variable load has been modeled in the d-q frame in terms of P and Q, given by Eqs. (3), (4) and shown in the block-diagram of Fig. 6 [34].

$$i_d = \frac{2}{3} \cdot \frac{v_d}{v_d^2 + v_q^2} \cdot P + \frac{2}{3} \cdot \frac{v_q}{v_d^2 + v_q^2} \cdot Q \quad (3)$$

$$i_q = \frac{2}{3} \cdot \frac{v_q}{v_d^2 + v_q^2} \cdot P - \frac{2}{3} \cdot \frac{v_d}{v_d^2 + v_q^2} \cdot Q \quad (4)$$

where P and Q are the desired active and reactive power of the responsive load, respectively, and v_d , v_q (i_d , i_q) are the load

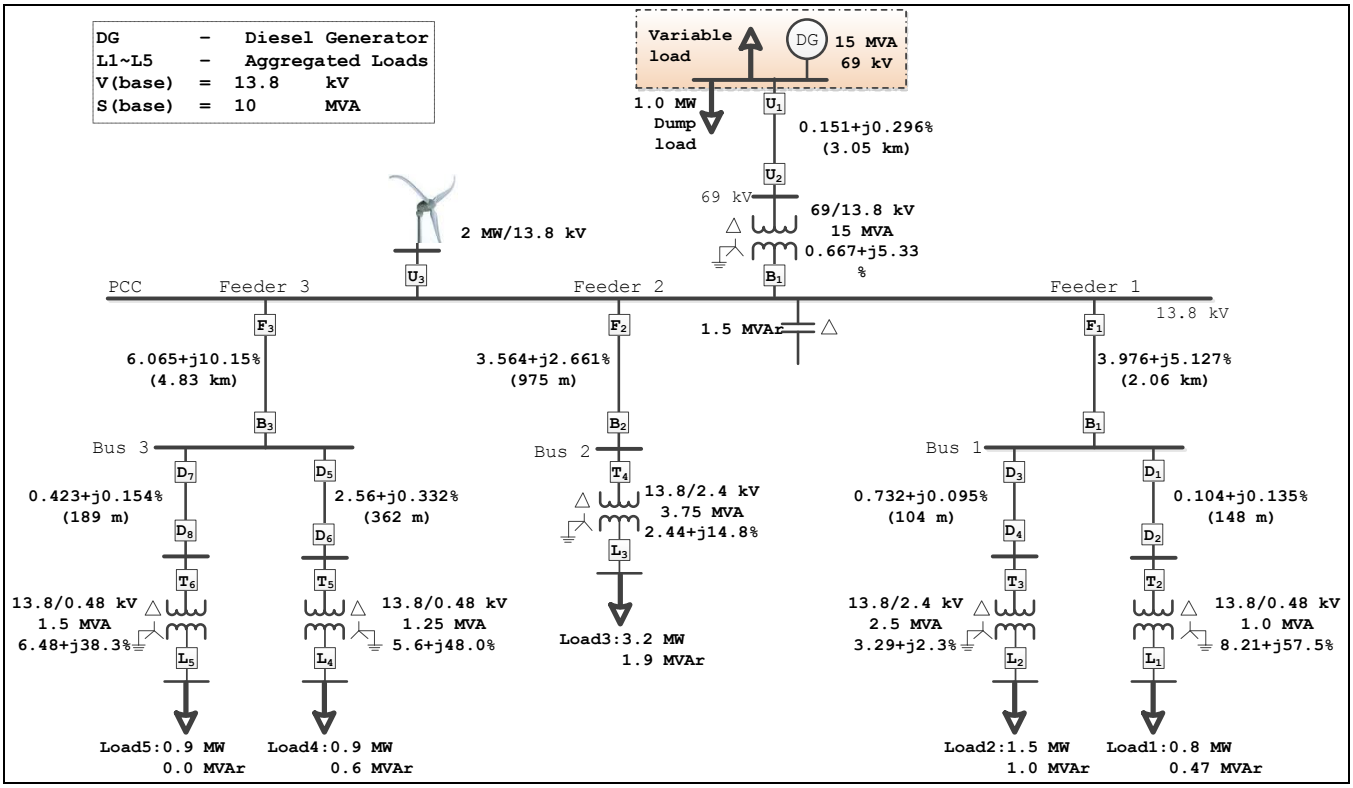

Fig. 5. Modified IEEE 13-bus standard distribution system schematic diagram.

voltage (current) in the *d-q* frame. To transform the values from the *abc* frame to the *d-q* frame and vice versa, a phase locked-loop (PLL) is applied [34]. The voltage values in the *d-q* frame are extracted from the actual voltage across the load through the "*abc* to *dq0* transformation" block. The *d*- and *q*-axis currents are then calculated and transformed into the *abc* frame through the "*dq0* to *abc* transformation" block.

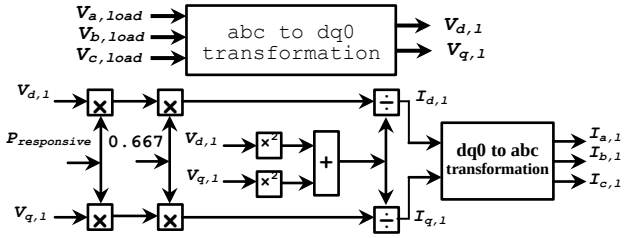

Fig. 6. Schematic of modeling of the active variable load.

Five aggregated loads (L_1-L_5) are shown in Fig. 5, where each one represents a DR aggregator, as shown in Fig. 1. Each aggregated load is divided into three different types: responsive, critical, and non-responsive. This categorization of the aggregated loads is shown in Fig. 7. The responsive loads are variable active loads, the amount of which is determined by the DR algorithm. The critical and non-responsive loads are modeled as constant impedance loads. In this study, a central controller is responsible for frequency regulation. The controller can be considered as a utility owned control facility which has direct access to the individual responsive loads in the utility's distribution network through two-way communication (with a pre-defined latency), i.e. smart grid era.

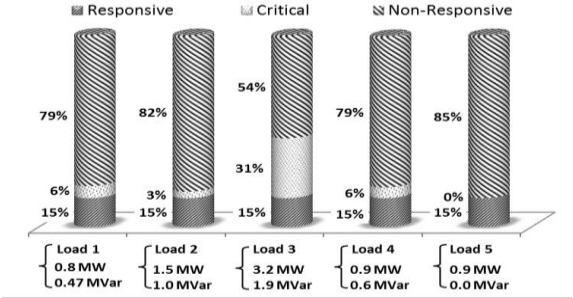

Fig. 7. The technical characteristic of the load in the test system.

IV. Simulation Results

In order to assess the effectiveness of the comprehensive controller (AHC + SBS) vs. the no-control and the AHC controller (alone) cases, several simulation experiments have been performed on the 13-bus distribution network, discussed in subsections A-D below. Each simulation has been carried out for the comprehensive controller, the AHC controller (alone), and the no-control case. No wind power is considered in subsections A and B to examine the impact of variations in load demand on the system frequency and voltage. Subsections C and D are devoted to assessing the impact of DR in the presence of variable wind power; load demand is kept constant in these cases.

A. Scenario I: Light loading– decrease in load (NO WIND)

In this case, Load 5 (0.9 MW) is disconnected at t=7 sec, and as a result, the system frequency increases, resulting in $\Delta f > 0.05$ Hz. The lower setpoint of the diesel generator torque is limited to 0.65 p.u. to prevent it from lowering the torque further to correct the frequency deviation under light loading. The light loading in conventional power system can be viewed as a condition where there are only base-load steam power plants available with limited capability for ramping up and down. In this situation, it is more convenient to add a dump load to the system instead of changing the output power of those power plants. This prevents mechanical and thermal stress on the generation units. In this study, a 1-MW dump load has been applied at the 69-kV bus to which the DG is connected (Fig. 5), to be activated once the frequency deviation exceeds 0.5 Hz, i.e. when the frequency cannot be stabilized through DR, or in the no-control case.

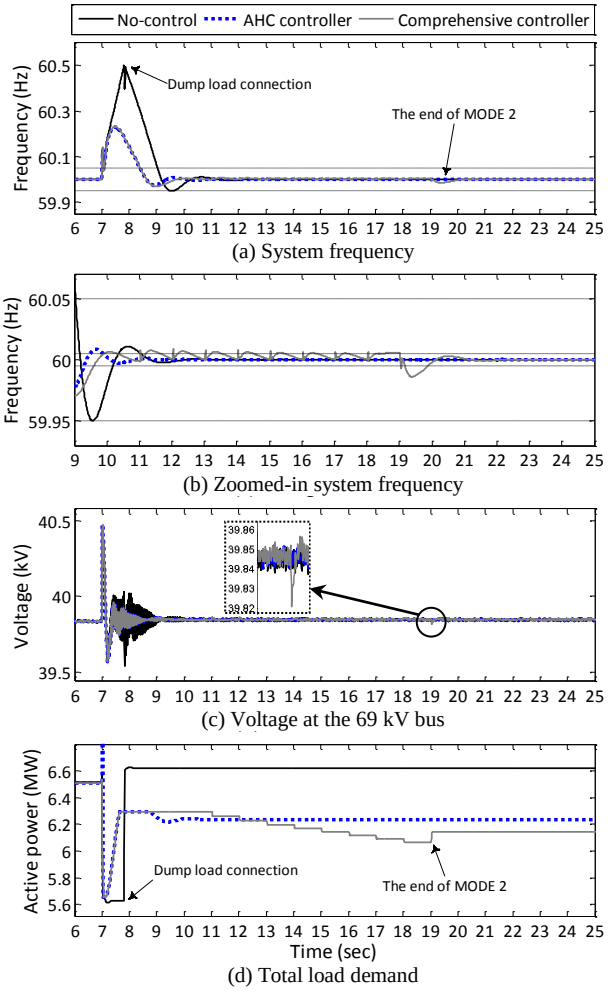

Fig. 8. Frequency, voltage, and total load demand: Light loading with no wind power generation.

In Fig. 8 the frequency variation, voltage and total power demand for the different DR approaches are compared with the no-control case. Fig. 8(a) and (b) show that both the DR approaches (AHC and comprehensive) bring the frequency to the desired range faster than the no-control case. The dump load is utilized to regulate the system frequency at around 7.8 sec in the no-control case. This happens when the frequency deviation exceeds 0.5 Hz to stabilize the frequency. When the SBS controller is active, frequency fluctuation is more in the range of ±0.005 Hz, which is safe for the system's operation.

These variations are shown in the zoomed-in frequency variation, Fig. 8(b). This figure also shows the time at which the SBS controller lowers the amount of the manipulated load to a minimum, which occurs approximately at 19 sec, when operation MODE 2 ends and the system will go to normal operation (MODE 0). As a result of frequency regulation, the system voltage is also stabilized faster, as shown in Fig. 8(c). Also, less voltage fluctuation is observed during the transient period, when the comprehensive controller and the AHC controller (alone) are applied. It is also noticed from this figure that the voltage remains in the acceptable range at the end of operation of the SBS controller at (t≈19 sec).

Fig. 8(d) illustrates the total demand on the system for the different cases. It can be seen that in the comprehensive approach a smaller percentage of responsive load has been manipulated at steady-state compared to the AHC approach. Under the comprehensive control the total load demand at steady-state is 6.142 MW and 77.38% of the responsive load is manipulated, whereas for the AHC controller the total load at stead-state is 6.238 MW and 91.77% of the responsive load is manipulated. This difference between the manipulated loads in the two cases corresponds to 14.39% savings when the comprehensive controller is used, which of course results in a higher customers' QoS.

Frequency regulation has been achieved in the no-control case with the aid of a 1-MW dump load, which is a waste of energy and not desirable. However, when the DR is applied, in addition to frequency and voltage regulation, it can also be effective in peak load shaving and load shifting.

B. Scenario II: Heavy loading– increase in load (NO WIND)

In this case, a 0.6-MW load is added to the 69-kV bus at t=7 sec, resulting in a negative frequency deviation. The upper setpoint of the mechanical torque of the diesel generator is limited to 0.96 p.u to prevent it from totally correcting the frequency deviation so that the effect of DR can be examined.

Fig. 9 shows the system frequency and voltage variations, and power demand under the different DR approaches and the no-control case. In the no-control case, as soon as the frequency deviation begins to exceed 0.5 Hz (Fig. 9(a)), it is brought back to within limits with unscheduled load shedding, which jeopardizes customers' QoS and is undesirable.

The frequency variation, given in Fig. 9 (a) and (b), shows that both the AHC and comprehensive DR approaches bring the frequency to its desired range faster than the no-control case. As shown in Fig. 9 (a), Load 5 on bus 3 (Fig. 5) is shed at around 8.7 sec because the frequency deviation falls below -0.5 Hz. For safe operation in the no-control case, Load 4 has been considered as backup emergency to be disconnected from bus 3 whenever the frequency deviation falls below -0.8 Hz. This condition didn't happen in this study.

In both the DR approaches, the frequency is stabilized through manipulating a small portion of the responsive loads – not by shedding the whole feeder, as in the no-control case. As shown in the zoomed-in Fig. 9 (b), when the SBS controller is in operation, the system frequency fluctuation is more (in the range of ±0.005 Hz) than when the AHC controller (alone) is operating. However, the fluctuations are small and the system is in the safe operation region. At around 33 sec, the SBS controller minimizes the amount of responsive loads needed to stabilize the frequency. At this time, the system goes to the no-control mode (MODE 0). As a result of frequency regulation, the voltage of the system is also stabilized, as shown in Fig. 9 (c). No considerable voltage fluctuation is observed at the end of MODE 2, when the SBS controller ends. The reason is the adaptive nature of the SBS controller, according to Eq. 2, which results in smaller step changes in the manipulated load at the end of MODE 2.

Fig. 9 (d) shows the total demand on the system for the no-control case, the AHC (alone), and the comprehensive control. In each case, the amount of system load that remains active at steady-state to keep the system frequency at 60 Hz is shown. The amount of load that remains active in each case is as follows: 6.27 MW under no-control, 6.756 MW with the AHC (alone), and 7.002 MW with the comprehensive controller. The percentage of manipulated responsive load in the case of AHC and comprehensive controller are 52.07% and 20.30%, respectively. It is clear that a larger amount of load remains active under the comprehensive control approach. The difference between the percentages of manipulated load at steady-state for the comprehensive approach compared to the AHC approach is 31.77%, which again results in improved QoS for the customers.

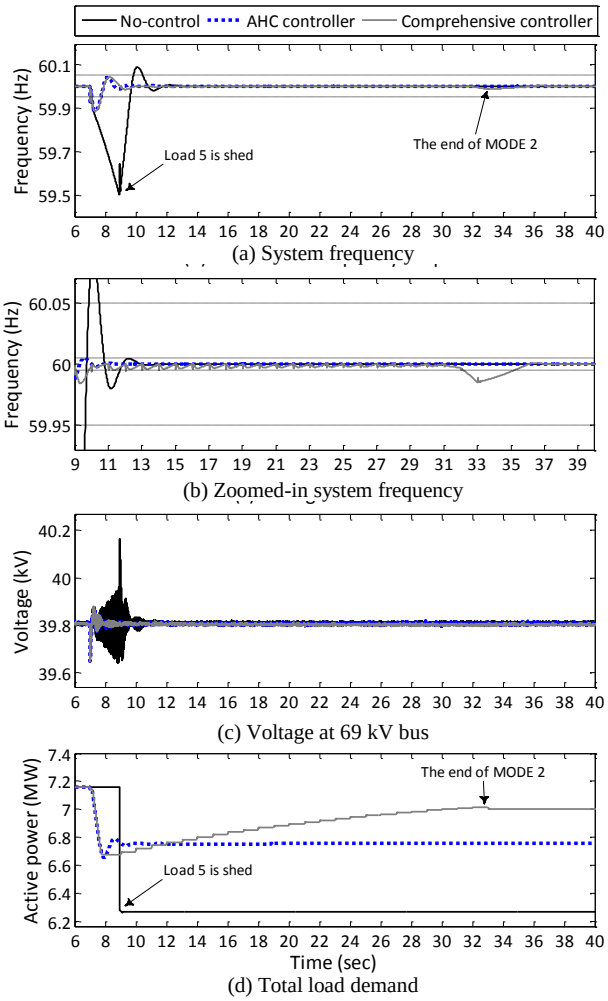

Fig. 9. Frequency, voltage, and total load demand: Heavy loading with no wind power generation.

C. *Scenario III: Excess wind power generation*

In this case, a 2 MW wind turbine is connected to the network at the PCC, as shown in Fig. 5. The system frequency, voltage, and power demand are shown in Fig. 10. At t=7 sec, the wind power suddenly increases from 0.6 MW to 1.3 MW. In the no-control case, a 1-MW dump load is activated at the PCC (increasing the total system load to almost 7.5 MW) once the system frequency reaches 60.5 Hz at approximately t=8.8 sec (Fig. 10 (a) and (b)). As shown in Fig. 10 (d), the total amount of load in the AHC and comprehensive cases at steady-state are: 7.037 MW and 6.778 MW, respectively. The percentages of manipulated responsive loads are 65.59% for the AHC and 33.04% for the comprehensive approach. This again shows the effectiveness of the comprehensive controller in manipulating (in this case activating) a smaller percentage of the responsive loads which translates to improved customers' QoS. In order to keep the system frequency at 60 Hz at steady-state, 32.55% of the responsive loads have been saved when the comprehensive controller is operating compared to when the AHC controller is applied.

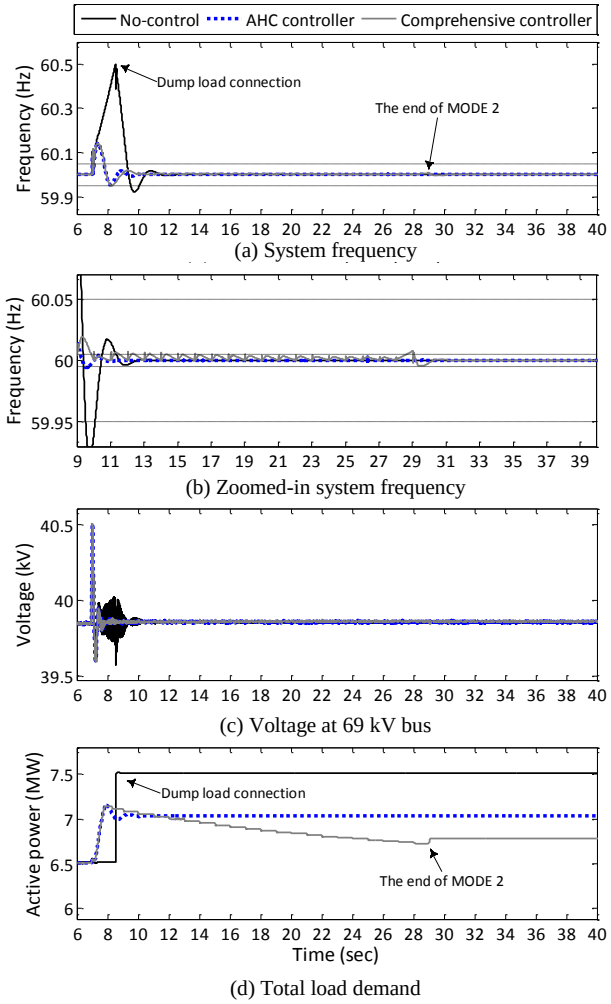

Fig. 10. Frequency, voltage, and total load demand: Excess wind power generation.

Fig. 10 (b) shows the zoomed-in frequency variation. In the case of comprehensive controller, the frequency varies within the acceptable range of 60±0.005 Hz until around t=29 sec, when it tends to go outside the limit. At this time, the SBS controller has accomplished the minimization of the manipulated responsive loads (i.e., the end of MODE 2). As shown in Fig. 10 (c), as a result of frequency stabilization the system voltage is also stabilized (in all cases).

D. *Scenario IV: Unexpected shortage in wind power generation*

In this scenario, the wind power generation suddenly decreases from 1.3 MW to 0.8 MW. In the no-control case, partial load shedding in load 5 (a non-critical load in Fig. 5) takes place as soon as the frequency falls to 59.5 Hz (Fig. 11 (a), (d)). Fig. 11 (d) also shows the total system power demand when the AHC and comprehensive control are applied. It is clear from this figure that at steady-state, more loads are active when the comprehensive controller is operating as compared to when the AHC (alone) is applied. In each case the percentage of manipulated load is 44.63% for the AHC and 11.35% for the comprehensive approach. The difference results in a savings of 33.28% of the responsive loads in the comprehensive controller case compared to the AHC controller (alone), which again translates to improved customers' QoS.

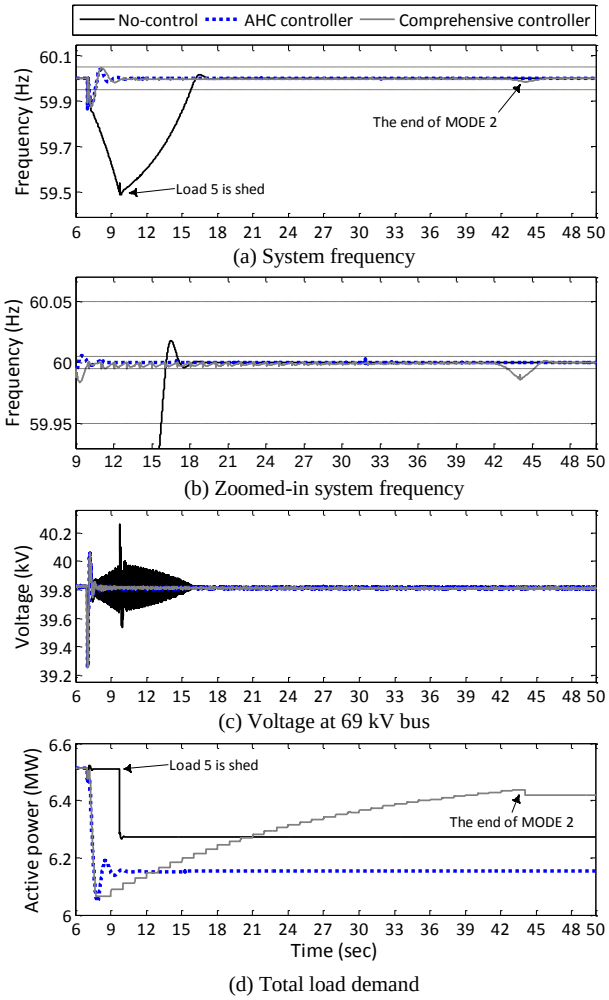

Fig. 11. Frequency, voltage, and total load demand: Unexpected shortage in wind power generation.

Fig. 11 (b) shows the zoomed-in frequency variation, and Fig. 11 (c) shows the system voltage profile. It is clear from this figure that voltage stabilizes faster when the AHC and comprehensive controller are operating.

V. Discussion

In an actual system, there are two possibilities of delay in the operation of the system; one is related to the dynamic response of the loads and the other related to the delay in communication. Both delays should be considered in the DR control algorithms to prevent unnecessary switching of the responsive loads. Purely resistive loads (such as EWHs), considered in our study, respond instantly to the variations in their input voltage. Therefore, it can be assumed that there is no delay in their response to the changes in the input signal [4]. However, communication delay, often referred to as latency, should be considered. Latency is the length of time from when a request is made by a control entity to when the electrical device receives the request and acts on it. With the existing internet infrastructure, latencies of around 500 msec are achievable [9]. We have evaluated the impact of different latencies (between 20 msec and 500 msec) on the performance of the comprehensive controller. Fig. 12 shows the frequency variation with different latencies under light loading. It is clear from this figure that the controller is able to regulate the frequency successfully for latencies of up to 300 msec. At the latency of 500 msec, the system frequency is unstable.

In all the simulation studies reported earlier, a wireless network with a latency of 20 msec is assumed as the communication protocol between the control entities and loads.

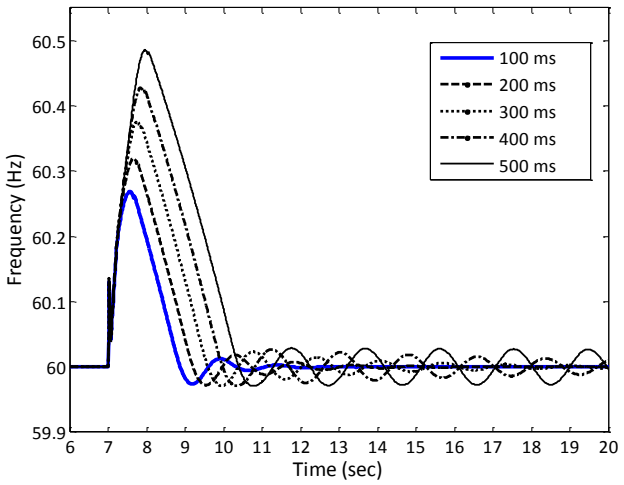

Fig. 12. System frequency with different latencies, light loading with comprehensive controller case.

In addition to the technical feasibility of the DR reported in this paper, a detailed cost-benefit analysis of the DR is also necessary to truly justify its deployment in the smart grid era. We have ongoing work on this topic, which will be reported in a follow-on paper.

VI. Conclusions

This paper presents a comprehensive DR strategy for frequency regulation in a microgrid with and without wind power generation. It has been shown through different scenarios that the proposed DR strategy is able to regulate the system frequency and voltage in a microgrid by:

1. The application of the AHC controller to reduce the frequency deviation after a sudden disturbance with maximum effort.
2. Minimizing the amount of manipulated responsive loads needed to keep the frequency within the desired range at steady-state, which improves customers' QoS.

The central DR strategy is based on communication between the utility control center and the responsive loads and has been shown to be stable up to a latency of 300 msec.

Appendix

The diesel generator specifications are given in Table I [32].

TABLE I
DIESEL GENERATOR PARAMETERS

Synchronous generator parameters	
Nominal power	15 MVA
Line-to-line voltage	69 kV
Nominal frequency	60 Hz
d-axis reactance (X_d, $X_{d'}$, $X_{d''}$)	1.305, 0.296, 0.252 p.u.
q-axis reactance (X_q, $X_{q'}$, $X_{q''}$)	0.474, 0.243, 0.18 p.u.
Inertia coefficient	2.2 sec
Governor and Diesel Engine parameters	
Regulator gain	40
Regulator time constants (T_1, T_2, T_3)	0.01, 0.02, 0.2 sec
Engine time delay	0.14 sec
Excitation controller parameters	
Regulator gain	200
Regulator time constants	0.02 sec
Damping filter gain and time constant	0.001, 0.1 sec

References

[1] U.S. Dept. of Energy, "Benefits of Demand Response in Electricity Markets and Recommendations for Achieving them," A report to U.S. Congress, Feb. 2006.
Web address: http://eetd.lbl.gov/ea/ems/reports/congress-1252d.pdf

[2] Federal Energy Regulatory Commission, "Assessment of Demand Response and Advanced metering," A report to U.S. Congress, Dec. 2008.
Web address: http://www.ferc.gov/legal/staff-reports/demand-response.pdf

[3] G.C. Heffner, C.A. Goldman, M.M. Moezzi, "Innovative Approaches to Verifying Demand Response of Water Heater Load Control," *IEEE Trans. on Power Del.*, vol. 21, no. 1, 2006, pp. 388–397.

[4] R. Jia, M.H, Nehrir, D.A. Pierre, "Voltage Control of Aggregate Electric Water Heater Load for Distribution System Peak Load Shaving Using Field Data," In *Proc.* 39th North American Power Symposium (NAPS), 2007, pp. 492–497.

[5] J. Kondoh, N. Lu, D.J. Hammerstrom, "An Evaluation of the Water Heater Load Potential for Providing Regulation Service," *IEEE Trans. on Power Syst.*, vol. 26, no. 3, 2011, pp. 1309–1316.

[6] N. Lu, S. Katipamula, "Control Strategies of Thermostatically Controlled Appliances in a Competitive Electricity Market," In *Proc.* Power Engineering Society General Meeting, vol. 1, 2005, pp. 202–207.

[7] R. Walawalkar, S. Blumsack, J. Apt, S. Fernands, "An Economic Welfare Analysis of Demand Response in the PJM Electricity Market," *Energ. Policy*, vol. 36, no. 10, 2008, pp. 3692–3702.

[8] M. Klobasa, "Analysis of Demand Response and Wind Integration in Germany's Electricity Market," *IET Renew. Power Gener.*, vol. 4, no. 1, 2010, pp. 55–63.

[9] A. Brooks, E. Lu, D. Reicher, C. Spirakis, B. Weihl, "Demand Dispatch: Using Real-Time Control of Demand to Help Balance Generation and Load," *IEEE Power Energy Mag.*, vol. 8, no. 3, 2010, pp. 20–29.
[10] J. Medina, N. Muller, I. Roytelman, "Demand Response and Distribution Grid Operations: Opportunities and Challenges," *IEEE Trans. on Smart Grid*, vol. 1, no. 2, 2010, pp. 193–198.
[11] H. Saele, O.S. Grande, "Demand Response from Household Customers: Experiences from a Pilot Study in Norway," *IEEE Trans. on Smart Grid*, vol. 2, no. 1, 2011, pp. 102–109.
[12] N. Ruiz, I. Cobelo, and J. Oyarzaabal, "A Direct Load Control Model for Virtual Power Plant Management," *IEEE Trans. on Power Syst.*, vol. 24, no. 2, 2009, pp. 959–966.
[13] A.J. Conejo, J.M. Morales, L. Baringo, "Real-Time Demand Response Model," *IEEE Trans. on Smart Grid*, vol. 1, no. 3, 2010, pp. 236–242.
[14] D.T. Nguyen, M. Negnevitsky, M. de Groot, "Pool-Based Demand Response Exchange—Concept and Modeling," *IEEE Trans. on Power Syst.*, vol. 26, no. 3, 2011, pp. 1677–1685.
[15] P. Faria, Z. Vale, J. Soares, J. Ferreira, "Demand Response Management in Power Systems Using a Particle Swarm Optimization Approach," *IEEE Intell. Syst.*, to be published, 2011.
[16] M. Parvania, M. Fotuhi-Firuzabad, "Integrating Load Reduction into Wholesale Energy Market with Application to Wind Power Integration," *IEEE Syst. J.*, vol.6, no. 1, 2012, pp. 35–45.
[17] K. Dietrich, J.M. Latorre, L. Olmos, A. Ramos, "Demand Response in an Isolated System with High Wind Integration," *IEEE Trans. on Power Syst.*, vol. 27, no. 1, 2012, pp. 20–29.
[18] N. Navid-Azarbaijani, M.H. Banakar, "Realizing Load Reduction Functions by Aperiodic Switching of Load Groups," *IEEE Trans. on Power Syst.*, vol. 11, no. 2, 1996, pp. 721–727.
[19] K.Y. Huang, H.C. Chin, Y.C. Huang, "A Model Reference Adaptive Control Strategy for Interruptible Load Management," *IEEE Trans. on Power Syst.*, vol. 19, no. 1, 2004, pp. 683–689.
[20] D. Westermann and A. John, "Demand Matching Wind Power Generation with Wide-Area Measurement and Demand-Side Management," *IEEE Trans. Energy Convers.*, vol. 22, no. 1, 2007, pp. 145–149.
[21] D. Trudnowski, M. Donnelly, E. Lightner, "Power-System Frequency and Stability Control using Decentralized Intelligent Loads," In *Proc.*, IEEE PES Conference and Exhibition Transmission and Distribution, 2005, pp. 1453–1459.
[22] J.A. Short, D.G. Infield, L.L. Freris, "Stabilization of Grid Frequency Through Dynamic Demand Control," *IEEE Trans. on Power Syst.*, vol. 22, no. 3, 2007, pp. 1284–1293.
[23] A. Molina-García, F. Bouffard, D.S. Kirschen, "Decentralized Demand-Side Contribution to Primary Frequency Control," *IEEE Trans. on Power Syst.*, vol. 26, no. 1, 2011, pp. 411–419.
[24] D. Angeli, P-A. Kountouriotis, "A Stochastic Approach to "Dynamic-Demand" Refrigerator Control," *IEEE Trans. on Control Syst. Technol.*, to be published, 2011.
[25] S.A. Pourmousavi, M.H. Nehrir, "Demand Response for Smart Microgrid: Initial Results," In *Proc.* 2nd IEEE PES Innovative Smart Grid Technologies (ISGT), 2011, pp. 1–6.
[26] S.A. Pourmousavi, M.H. Nehrir, C. Sastry, "Providing Ancillary Services through Demand Response with Minimum Load Manipulation," In *Proc.* North American Power Symposium (NAPS), 2011, pp. 1–6.
[27] M.H. Albadi, E.F. El-Saadany, "A Summary of Demand Response in Electricity Markets," *Electr. Pow. Syst. Res.*, vol. 78, no. 11, 2008, pp. 1989–1996.
[28] Y.G. Rebours, D.S. Kirschen, M. Trotignon, S. Rossignol, "A Survey of Frequency and Voltage Control Ancillary Services-part I: Technical Features," *IEEE Trans. on Power Syst.*, vol. 22, no. 1, 2007, pp. 350–357.
[29] North American Electric Reliability Corporation, "Standard BAL-004-0 - Time Error Correction," Apr. 2005. Available online: http://www.nerc.com/files/BAL-004-0.pdf
[30] F. Katiraei, M.R, Iravani, P.W. Lehn, "Micro-Grid Autonomous Operation During and Subsequent to Islanding Process," *IEEE Trans. on Power Del.*, vol. 20, no. 1, 2005, pp. 248–257.
[31] V. Menon, M.H. Nehrir, "A Hybrid Islanding Detection Technique Using Voltage Unbalance and Frequency Set Point," *IEEE Trans. on Power Syst.*, vol. 22, no. 1, 2007, pp. 442–448.
[32] MATLAB/Simulink SimPowerSystems Documentation, Available on line: http://www.mathworks.com/
[33] *IEEE Recommended Practice for Excitation System Models for Power System Stability Studies*, IEEE Standard 421.5, 2005.
[34] A. Yazdani, R. Iravani, *Voltage-Sourced Converters in Power Systems: Modeling, Control, and Applications*, Hoboken, NJ, John Wiley & Sons Inc., 2010, ch. 4.

BIOGRAPHIES

S. Ali Pourmousavi (S'07) received the B.S. degree with honors from University of Mazandaran, Iran in 2005 and M.S. degree with honors from Amirkabir University of Technology (Tehran Polytechnic), Iran in 2008, all in electrical engineering. He is a Ph.D. student in the Electrical and Computer Engineering (ECE) Department at Montana State University, Bozeman, MT. His research interests include energy management of hybrid power generation systems, load control and demand response, and wind speed and power forecasting.

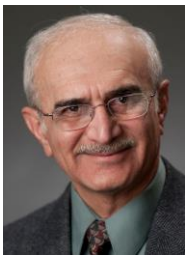

M. Hashem Nehrir (S'68–M'71–SM'89–F'10) received the B.S., M.S., and Ph.D. degrees from Oregon State University, Corvallis, in 1969, 1971, and 1978, respectively, all in electrical engineering. He was with the Electrical Engineering Department, Shiraz University, Iran from 1971 to 1986. Since 1987, he has been on the faculty of the Electrical and Computer Engineering Department, Montana State University, Bozeman, MT, where he is a Professor. His research interests include modeling and control of power systems, alternative energy power generation systems, and application of intelligent controls to power systems. He is the author of three textbooks and an author or coauthor of numerous technical papers.